Journal of Computational Electronics 3: 397–400, 2004

Simulation Schemes in 2D Nanoscale MOSFETs: A WKB Based Method

C. NEGULESCU, N. BEN ABDALLAH AND E. POLIZZI
Mathématiques pour l'Industrie et la Physique, UMR CNRS 5640,
Université Paul Sabatier, 118, route de Narbonne, F-31062 Toulouse Cedex, France
negulesc@mip.ups-tlse.fr
naoufel@mip.ups-tlse.fr
epolizzi@ecn.purdue.edu

M. MOUIS
IMEP (UMR CNRS/INPG/UJF), 23 rue des Martyrs, BP 257, F-38016 Grenoble Cedex, France
mouis@enserg.fr

Abstract. The WKB approximation is used in this paper to develop a model simulating nanoscale MOSFETs with a reduced numerical cost. The method is based on the Schrödinger-Poisson approach with open boundary conditions (QTBM). Accurately results have been obtained with significantly gain in simulation time.

Keywords: Schrödinger-Poisson equation, WKB approximation, nanoscale DG NMOSFETs

1. Introduction

In this paper we present an accelerated numerical method to simulate quantum ballistic transport in Silicon ultrashort channel MOSFETs. There is a great amount of work (see References) dedicated to semiconductor device simulation, either by finite element/difference methods or by Green's function formalism. The present approach is implemented in an improved version of the NESSIE code, which was originally developed in the MIP laboratory. It consists in a finite element resolution of the Schrödinger equation with quantum transmitting boundary conditions [8], coupled to the Poisson equation for the electrostatic potential. The method exposed here aims at reducing significantly the simulation time by reducing the number of grid points, while keeping a good accuracy. For this purpose, the WKB approximation is introduced in the subband decomposition method [3], allowing the construction of an original finite element scheme. Detailed features of this method are presented in [1,9].

2. Method

We seek a 2D solution of the self-consistent Schrödinger equation with open boundary conditions (current carrying), coupled to the Poisson equation.

Step I. Subband decomposition (SDM)

Assuming the electron gas being confined in the direction z, we consider the decomposition of the 2D wave function

$$\psi_\epsilon(x,z) = \sum_i \varphi_\epsilon^i(x)\chi_i(z;x). \tag{1}$$

with φ_ϵ^i the longitudinal wave functions and χ_i the transversal ones. The resolution of the Schrödinger equation in the whole 2D domain

$$-\frac{\hbar^2}{2}\frac{1}{m_x(z)}\Delta_x\psi_\epsilon(x,z) - \frac{\hbar^2}{2}\frac{\partial}{\partial z}\left(\frac{1}{m_z(z)}\frac{\partial}{\partial z}\psi_\epsilon(x,z)\right) + V(x,z)\psi_\epsilon(x,z) = \epsilon\psi_\epsilon(x,z) \tag{2}$$

is thus replaced by the resolution of 1D eigenvalue problems in the confined direction z, Eq. (3), and many coupled 1D Schrödinger equations projected on the transport direction x, Eq. (4)

$$-\frac{\hbar^2}{2}\frac{\partial}{\partial z}\left(\frac{1}{m_z(z)}\frac{\partial}{\partial z}\chi_i(z;x)\right)+V(x,z)\chi_i(z;x) = E_i(x)\chi_i(z;x), \quad \int_0^1 |\chi_i(z;x)|^2 dz = 1 \tag{3}$$

$$-\frac{d^2}{dx^2}\varphi_\epsilon^i(x) - 2\sum_{j=1}^{\infty} a_{ij}(x)\frac{d}{dx}\varphi_\epsilon^j(x) - \sum_{j=1}^{\infty}\left(b_{ij}(x)+\frac{2}{\hbar^2}c_{ij}(x)(\epsilon - E_j(x))\right)\varphi_\epsilon^j(x) = 0, \tag{4}$$

where the full 2D nature of the problem results in additional coupling terms which have been fully accounted for in the work presented here. The number of unknowns is thus reduced from $N_x \times N_z$ for the standard method to $N_x \times M$ for the SDM method, where M is the number of subbands taken into consideration, N_x resp. N_z the number of grid points in the transport resp. confined direction.

Step II. WKB approximation (SDM/WKB)

Using oscillating interpolation functions instead of polynomial ones for the resolution of the 1D Schrödinger Eq. (4), enables us to reduce significantly the number of grid points in the x-direction. To simplify, we shall expose here the WKB approximation to the 1D case, the coupling terms reducing thus to $a_{ij} = b_{ij} = 0$ and $c_{ij} = \delta_{ij}m$. The 2D case is treated in detail in [1,9]. Starting from the Ansatz

$$\varphi(x) = \alpha(x)e^{\mathrm{i}S(x)/\hbar},$$

the wave function reads in an interval (x_0, x_1) far from a turning point

$$\varphi(x) = \begin{cases} \dfrac{1}{\sqrt[4]{2m(E-V(x))}}\left(Ae^{\frac{\mathrm{i}}{\hbar}S(x)} + Be^{-\frac{\mathrm{i}}{\hbar}S(x)}\right), \\ \qquad\qquad \text{for} \quad E - V(\cdot) > \delta \\ \dfrac{1}{\sqrt[4]{2m|E-V(x)|}}\left(Ae^{\frac{1}{\hbar}S(x)} + Be^{-\frac{1}{\hbar}S(x)}\right), \\ \qquad\qquad \text{for} \quad E - V(\cdot) < -\delta. \end{cases} \tag{5}$$

where $S(x) := \int_{x_0}^{x}\sqrt{2m|E-V(t)|}dt$ and $\delta > 0$ is a treshold value. Close to a turning point, i.e. $|E - V(x)| < \delta$, a matching procedure is required to determine the entire wave function. Some simple calculus permit us to express φ by means of the so-called WKB basis functions. The discretization method is then a finite volume method, where we replace the piecewise linear hat functions, corresponding to the nodal points, by the WKB basis functions. The quantum transmitting boundary conditions are naturally taken into account in this method. The WKB basis functions, represented in Fig. 1, oscillate with a frequency close to that of the wave function and in the limit $\Delta x \ll \lambda$ (de Broglie wavelength) reduce to usual linear interpolation functions. Accurate results have been obtained with much coarser grids and reduced computational time.

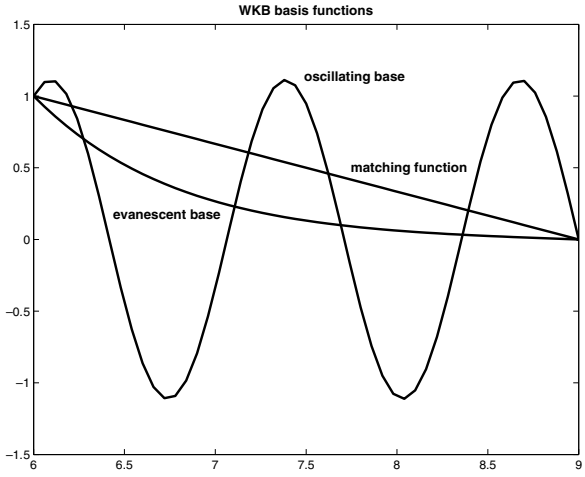

Figure 1. WKB basis functions.

3. Numerical Results

The results presented in this section are calculated with the improved version of the NESSIE simulator.

Device Structure

We simulated a Double-Gate NMOSFET with a channel length and a body thickness of 10 nm. The channel was assumed to be undoped (10^{16} cm^{-3} residual doping level), whereas the doping level of the included reservoirs (source and drain) was 10^{20} cm^{-3}. We accounted for the 6-fold degeneracy of the Si-conduction band and used the effective mass approximation ($m_T = 0.19 * m_e, m_L = 0.98 * m_e$) to describe the ellipsoidal symmetry of each band. This was sufficient here, due to the small bias voltages needed at such

short gate length. The oxide thickness was 1 nm. A finite barrier height (3e V) was assumed between Si and SiO_2, allowing the penetration of the wave functions in the gate oxide.

Numerical Efficiency

An extensive comparison between the two methods SDM and SDM/WKB has been performed to illustrate the efficiency of the new method. As an example, we show in Fig. 2(a) a plot of the sheet charge densities versus X and in Fig. 2(b) cross-sections of the potential energy along the channel, near the Si/SiO_2 interface. The agreement between full lines (SDM/WKB) and broken lines (SDM) is excellent. The SDM/WKB method approximated accurately the solution of the Schrödinger-Poisson equation with a mesh of only 20 points in the transport direction, whereas the SDM method used 72 grid points. The simulation time with the SDM/WKB method was significantly reduced by a factor of about 2.5 compared with the SDM method. To conclude, the WKB approximation has been successfully used in a SDM method to further reduce computation time and allow extensive simulation of 2D quantum transport in nanoscale MOSFETs of arbitrary geometry.

Physical Discussion

The following results are now obtained with the SDM/WKB method. Solution of the above mentioned equations allows the calculation of the 2D self-consistent potential and of the spatial distribution of microscopic quantities such as the 2D concentration of electrons according to position $n(x, z)$, its decomposition in the different subbands (including the distinction between primed and unprimed subbands, associated to the different valley orientations) and, if needed, a further decomposition according to injection energy at the contact. They allow the calculation of the 2D distribution of mean quantities, such as velocity $\vec{v}(x, z)$, kinetic energy $\epsilon(x, z)$, current density $\vec{j}_{m_x,m_y,m_z}(x, z)$ for each valley orientation, as well as the total current density $\vec{j}(x, z)$, etc.. Of course macroscopic quantities such as source and drain currents can be derived as well. For instance, Fig. 3 shows the drain characteristics obtained for a 10 nm thick film (z direction) and a 10 nm channel length (x direction). The results are given per unit length in the y-direction.

The repartition of the current between the three valley orientations shows interesting features as both the

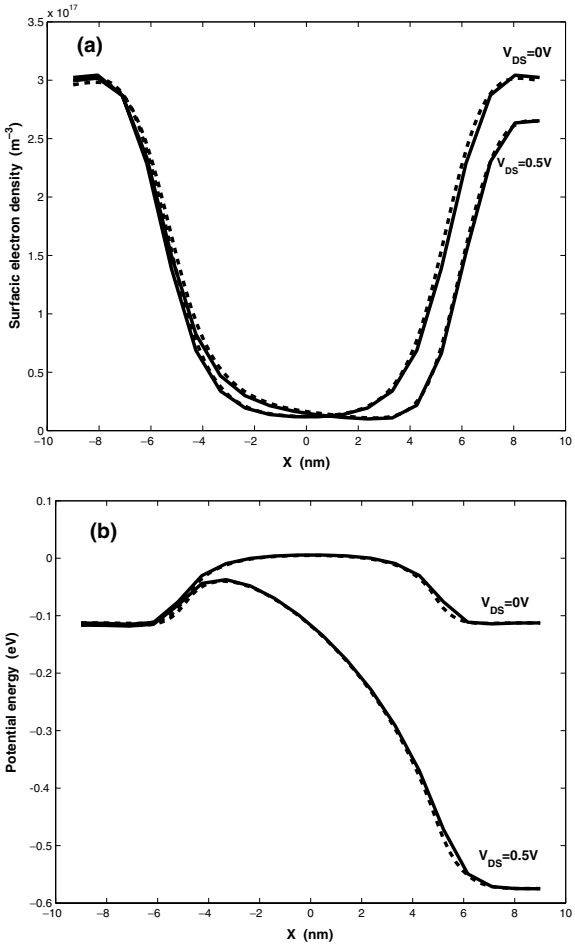

Figure 2. (a) Plot of the sheet charge density for $V_{GS} = 0.1$V. Full lines: SDM/WKB; Broken lines: SDM (b) Cross sections of the potential energy at 1 nm from the interface Si/SiO_2 for $V_{GS} = 0.1$ V.

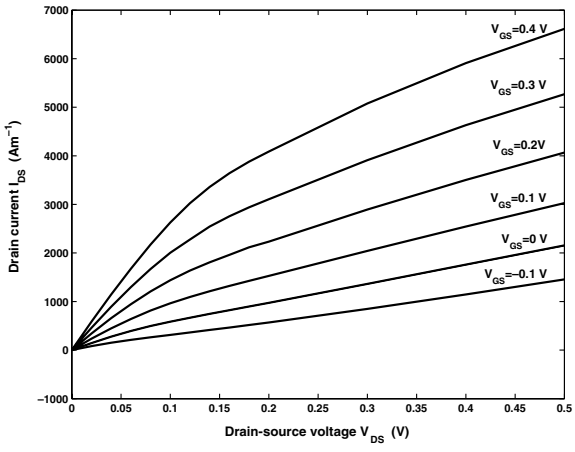

Figure 3. Current-Voltage output characterisctics for different gate voltages.

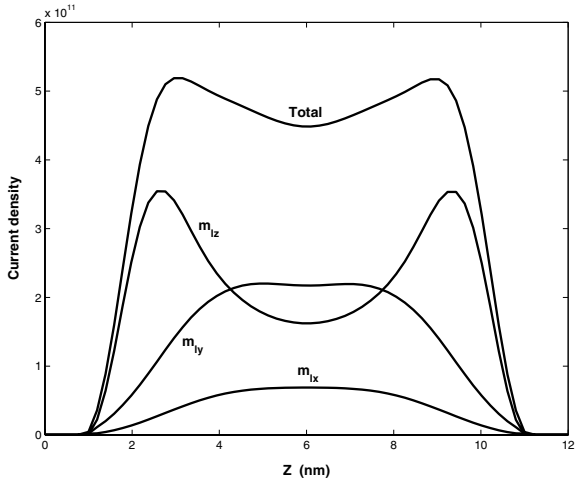

Figure 4. Cross sections of the current densities $\vec{j}_x$ close to the drain for $V_{\mathrm{DS}} = 0.5$ V and $V_{\mathrm{GS}} = 0.2$ V.

spatial variation of the current density and the amplitude are affected by the valley orientation (Fig. 4). Moreover, this method has the advantage of accounting for quantum effects in both directions, the confinement as well as the transport one. It is therefor able to analyse tunneling effects between source and drain. For instance, Fig. 5 shows how the energy spectrum of the electrons injected from the source in the first unprimed subbands (m_L in the confinement direction) evolves along the channel. This spectroscopy has been done for a low V_{GS} bias voltage and medium drain voltage. It shows that the leackage current which flows through the device is strongly influenced by electrons which

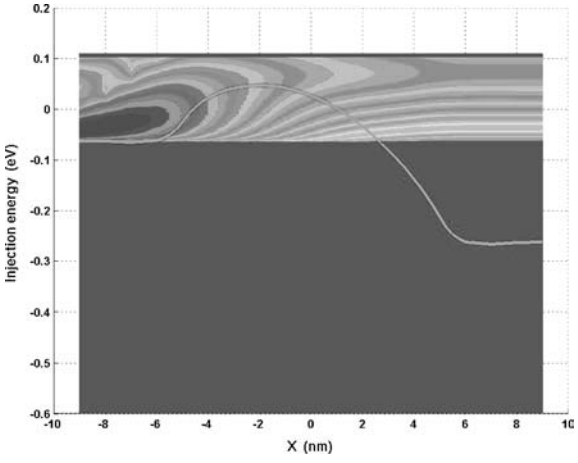

Figure 5. Source-injected electron population (configuration $m_x = m_L$) in log. scale and the tunneling effect beneath the potential barrier (green line) for $V_{\mathrm{DS}} = 0.2$ V and $V_{\mathrm{GS}} = -0.3$ V.

are tunneling through the source/channel barrier. This tunneling current leads to a larger drain induced barrier lowering (DIBL), as extracted from current voltage characteristics, compared to the internal barrier modulation by drain voltage. In particular, the barrier lowering is of the order of 25–27 meV when the drain voltage increases from 0.2 to 0.5 V. This leads, at a temperature of 300 K, to a current increase by a factor of 2.63. The transfer characteristics show however a current variation of a factor of about 4.05. This discrepancy is due to the tunneling of electrons through the source/channel barrier. These tunneling electrons bring a non negligible contribution to drain current compared to electrons injected thermionically above the barrier. The important point in our method is that no assumption is needed about the 2D shape of the barrier to evaluate this tunnelling contribution.

Acknowledgments

This research was supported by the project ACINIM 176-2004 "MOQUA", funded by the French Ministry of Research.

References

1. N. Ben Abdallah and C. Negulescu, "The WKB approximation for the modelling of quantum ballistic transport in nanoscale MOSFETs," in preparation.
2. N. Ben Abdallah and O. Pinaud, "Improved simulation of open quantum systems: resonances and WKB interpolation schemes," submitted to *J. Comp. Phys.*
3. N. Ben Abdallah and E. Polizzi, "A general quantum subband decomposition method for the modeling of electron transport in the ultimate devices," to appear in *J. Comp. Phys.*
4. S. Datta, "Nanoscale device modeling: the green's function method," *Superlattices and Microstructures*, **28**, 253 (2000).
5. M.V. Fischetti, "Theory of electron transport in small semiconductor devices using the Pauli master equation," *J. Appl. Phys.*, **83**, 270 (1998).
6. M.V. Fischetti, *Phys. Rev. B*, **59**, 4901 (1999).
7. G. Klimeck, F. Oyafuso, T.B. Boykin, R.C. Bowen, and P. von Allmen, *Computer Modeling Eng. Sci. (CMES)*, **3**, 601 (2002).
8. C.S. Lent and D.J. Kirkner, "The quantum transmitting boundary method," *J. Appl. Phys.*, **67**, 6353 (1990).
9. C. Negulescu, N. Ben Abdallah, and M. Mouis, "An accelerated algorithm for ballistic quantum transport simulations in 3D nanoscale MOSFETs," in preparation.
10. E. Polizzi and N. Ben Abdallah "Self-consistent three dimensional models for quantum ballistic transport in open systems," *Phys. Rev. B*, **66**, 245301 (2002).
11. A. Svizhenko, M.P. Anantram, T.R. Govindan, and B. Biegel, in *Device Research Conference 2001* (IEEE, Piscataway, NY 2001), p. 167.